ACS APPLIED NANO MATERIALS

www.acsanm.org Article

Electrically Controlled Nanofluidic DNA Sluice for Data Storage Applications

Nagendra Athreya, Apratim Khandelwal, Xiuling Li, and Jean-Pierre Leburton*

Cite This: *ACS Appl. Nano Mater.* 2021, 4, 11063−11069 Read Online

ACCESS | Metrics & More | Article Recommendations | Supporting Information

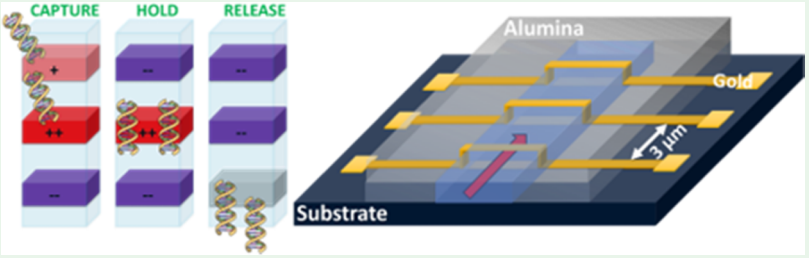

ABSTRACT: We propose an advanced architecture of an electrically controlled nanofluidic sluice for a DNA-based data storage device. Our device comprises embedded gold electrodes to which appropriate voltages are applied for effective capture, hold, and release of chimeric DNA strands. Electrostatic potential profiles across the device obtained *via* multiphysics simulation that solves for the Nernst−Planck−Poisson equation show nanoscale sluice operation for two device architectures: one with planar electrodes and the other with buried arch electrodes in combination with planar electrodes. Our simulations show that apart from its compatibility with complementary metal oxide−semiconductor (CMOS) technology, the device architecture with buried arch electrodes can effectively store the chimeric DNA strands without any leakage in conjunction with release on demand while offering the capability for large-scale integration.

KEYWORDS: *lab-on-a-chip data storage, chimeric DNA, nanofluidics, nanotunnel buried arch electrodes, multiphysics simulation*

INTRODUCTION

One of the most promising avenues in the quest of ultradense storage systems is macromolecular data storage,[1] in which DNA molecules stand out as primary candidates for massive storage media because of well-developed accompanying DNA "writing" (DNA synthesis)[2−7] and "reading" technologies (high-throughput DNA sequencing).[8−11] Furthermore, DNA and its derivatives are the only known macromolecules that enable random access[12,13] to select parts of the information content and large-scale amplification *via* polymerase chain reactions (PCRs).[14] DNA has also shown to lend itself to portable storage architectures with controllable data access, rewriting, and management, all in the presence of a large number of insertion−deletion errors inherent to inexpensive nanopore sequencers.[15,16] Recently, most research works have been geared toward DNA-based storage systems[2,3,5,14,17−20] with very little attention to addressing the most prominent challenges encountered in all practical implementations of DNA-based data storage systems, i.e., the excessively high cost and delay of DNA synthesis and the incompatibility of DNA media with the existing silicon computing architectures that support data access, retrieval, and computing. Additionally, even though native DNA-based data storage represents a significant paradigm shift in the area of polymer-based data storage in terms of reducing the recording cost by at least 2−3 orders of magnitude, several problems remain to match the cost−density performance and functional diversity of native storage and modern memory systems such as flash.[21]

To mitigate the issue of costly DNA synthesis and cost−density performance, the use of chimeric native DNA storage (synthetic polymers instead of DNA strings as recording media), in which native DNA bases are modified in different ways to increase component diversity, has been proposed.[18,22−24] Yazdi et al. were able to show that the use of chimeric DNA data storage over DNA synthesis-based storage reduced the cost from ∼$12 000 to ∼$4000 while increasing the information density from $\sim 10^{15}$ to 5×10^{20} B/g.[14] Another exciting avenue to cut down synthesis costs is to "reuse" the DNA strings by changing their structure rather than their content, which can be accomplished using nicking-based storage.[16,18,25] Recently, it has been shown that the cost to store a single bit of information using nicked-DNA is 6×10^{-5} compared to $0.07 via DNA synthesis.[18] Furthermore, to

Received: August 16, 2021
Accepted: October 4, 2021
Published: October 12, 2021

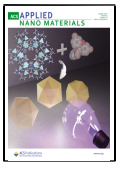

https://doi.org/10.1021/acsanm.1c02519
ACS Appl. Nano Mater. 2021, 4, 11063−11069

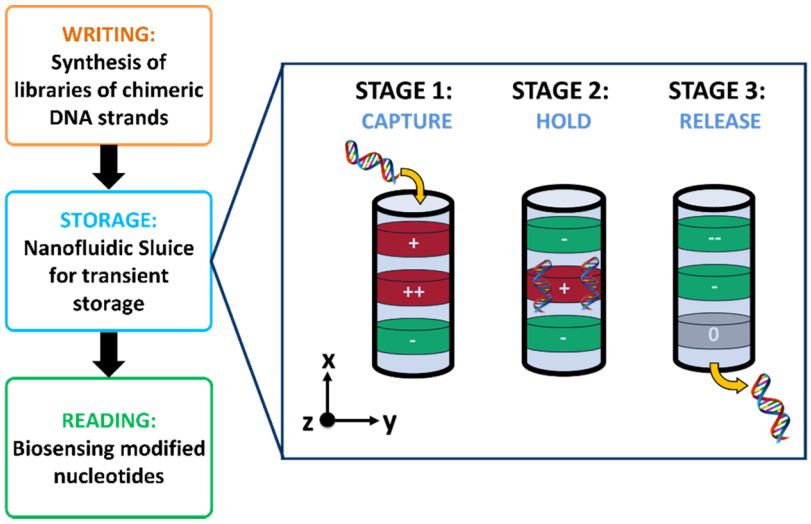

Figure 1. (Right) The three steps of the proposed methodology of DNA data storage system. (Left) schematics of the device architecture with the three sluice operation stages of effective capture, release, and hold of chimeric DNA strands.

make the resulting memories portable for operation in real-time, reading sequencers need to be integrated with the storage, random access, and readout circuitry. One main challenge in this area is to determine the biodevice architectures enabling the detection of chemical changes in chimeric DNA and structural changes such as DNA nicks. In this perspective, the use of solid-state nanopore FETs, for instance, would offer an attractive solution as they also provide seamless integration to complementary metal oxide−semiconductor (CMOS) devices.[10,11,18,25−27]

As native DNA storage requires random access to be performed *via* PCR reactions, a preferable solution consists of developing electronic circuits capable of accessing select DNA strands directly in real-time. Such solutions require maintaining specific DNA sequence data structures in different compartments for electrical access, none of which are currently available.

In this paper, a novel design of an integrated semiconductor−synthetic biology storage system centered around flexible grids of nanochannel structures with controlled three-dimensional (3D) nanoelectrodes that enable DNA string access and transfer, sample preparation, and controlled sequencing is proposed. One of the main features of this biodevice is its capability to address the main challenge of DNA compatibility with the existing silicon-based computing architectures integrated with solid-state nanopore sensors, for instance.

To validate our design, we model and simulate these lab-on-chip devices using COMSOL finite element modeling software. The multiphysics simulation couples the continuity equation for concentration of ion species in the electrolyte with Poisson's equation described for electric potentials (detailed description in the Methods section). The electric potentials and electric fields are obtained for different electrolytic concentrations in the channel.

The key ingredients of this system are planar, multilayered, patterned surface structures mostly made of components widely used in integrated circuits, which allow for the formation of grids of nanochannels or nanometer-scale tunnels.[28,29] This type of electronic system makes it possible to distribute chimeric DNA into different tunnels according to its content, perform property testing such as DNA concentration queries, and transport DNA to nanopore sequencing units, all in real-time and in larger volumes. The "on-chip" may be adapted to operate on RNA, proteins, or cellular complexes, as all these macromolecules contain electric charges.

Nanofluidic Sluice Device for Data Storage. Figure 1 (left) shows the end-to-end schematic of an effective DNA data storage system, where the data is encoded by synthetically modifying the nucleotides on native DNA strands (referred to as chimeric DNA strands). Libraries of different chimeric DNA strands are synthesized simultaneously and stored separately until a particular library is accessed and read *via* sensing of the modified nucleotides.

Here, we focus our analysis on modeling and validating the novel integrated semiconductor−synthetic biology storage system to effectively capture, hold, and release the chimeric DNA strands, as a nanoscale sluice operation illustrated in Figure 1 (right). The nanofluidic channel encases three electrodes to provide a uniform and concentrated electric field profile inside the channel for manipulating the negatively charged DNA molecules. Sequence loading and selection are accomplished *via* individually addressable embedded 3D electrodes that deterministically guide DNA into channels or release DNA in the microfluidic channel sequencing system. For example, one may encode images on chimeric DNA and guide the DNA content of each individual image into a separate nanochannel by changing the voltage at the electrodes. When a user demands a specific image, the electrode potential in the corresponding nanochannel is adjusted to enable the controlled release of a specific concentration of chimeric DNA. This DNA is subsequently guided through an on-chip sample preparation structure that denaturizes and linearizes the DNA, which is, in turn, guided to a specialized reading sequencer optimized for the detection of structural changes in DNA nucleotides. The solid-state sequencer also operates with prior information (the template DNA is known) and considerable redundancy (the chemical modification in each nucleotide within one synthetic oligo is the same).

Hence, the proposed nanofluidic sluice works in a three-stage process (Figure 1, right). The first stage "captures" the library of chimeric DNA strands into the desired nanochannel.

https://doi.org/10.1021/acsanm.1c02519
ACS Appl. Nano Mater. 2021, 4, 11063−11069

For this purpose, a positive voltage is applied to the first and middle electrodes so that inherently negative DNA molecules are attracted inside a particular channel by these positively charged electrodes. Simultaneously, a negative voltage at the last electrode retains the DNA inside the channel. The second stage "holds" the entire library of DNA until it is accessed for usage. For this purpose, the first electrode is negatively biased to repel the DNA further inside the channel while a higher voltage is applied to the middle electrode for the DNA to be maintained in the middle of the channel. Finally, in the last stage of "release", when a library of chimeric DNA strands is about to be accessed, negative voltages are applied to the first and middle electrodes while the last electrode is turned off to drive the DNA strands out of the channel toward a reading component comprised of a sequencer, such as a solid-state nanopore to detect the structural changes of the chimeric DNA strands rather than exact base calling. The release process mentioned here is a one-time process as the original library is expelled out of the nanochannel when accessed to be read. To restore the integrity of the original DNA library, one can envision two solutions: (1) to re-introduce the original library to be captured into the same tunnel after the release step and/or (2) given the versatility of the CMOS design techniques, one can achieve a massive array of these channels. This offers the advantage of storing multiple copies of the same library in many nanochannels.

Furthermore, in an array of nanochannels aimed at storing different libraries of chimeric DNA strands, each library is guided into a particular tunnel by applying a positive voltage to the electrodes at that channel's entrance. During this time, other tunnels are either performing "hold" or release operations where negative voltages are applied to the electrodes at the channel's entrance, repelling the library of the chimeric DNA strands that is to be stored and driving them toward the channel with a positively biased first electrode channel performing the "capture" operation.

The dynamics of the above-mentioned macromolecular system are governed by a combination of forces, among which electrostatic forces play an especially important role as biomolecules possess charges, and their atoms interact over distances of several angstroms.[30] Furthermore, phenomena caused by variations in pH levels and salt concentrations are primarily of electrostatic origin. Hence, to effectively manipulate the flow of DNA under the influence of the electric field, the consideration of screening effects of ions around the electrodes, characterized by the Debye length, λ_D (eq 1), is central to the nanoscale sluice operation

$$\lambda_D = \sqrt{\frac{K_B T \varepsilon_r \varepsilon_o}{2e^2 c_{bulk}}} \quad (1)$$

where T is the temperature, K_B is the Boltzmann constant, e is the elementary charge, c_{bulk} is the electrolyte bulk concentration, ε_o is the relative permittivity of free space, and ε_r is the solvent relative permittivity. Depending on the salt concentrations, the screening length spreads from a few angstroms to just over a few nanometers away from the electrodes, which imposes constraints on the nanofluidic channel design to efficiently retain or release the DNA molecules in the sluice operation. Hence, the diameter of the nanofluidic channels would be a critical parameter to optimize along with the electrolyte concentration for effective DNA storage. It is well known that DNA strands stored in an electrolyte such as TE buffer (Tris−HCl, ethylenediamine tetraacetic acid (EDTA), pH 8.0) at 1 or 10 mM concentrations remain undegraded and intact for more extended periods of time (tens of years).[17,31−34] From eq 1, one can assert that for a reasonably low concentration of 1 mM solution, the channel feature sizes of the order of ∼80−100 nanometers to electrically control the chimeric DNA strands would be optimum.

RESULTS AND DISCUSSION

Nanotunnel Structure Design. At this stage, the fabrication of cylindrical channels with nanoscale feature size covered with embedded electrodes for sluice operation is a challenging process. Instead, silicon nitride or alumina-based nanotunnels with flat rectangular cross sections, as shown in Figure 2, are easier to fabricate and, given their planar

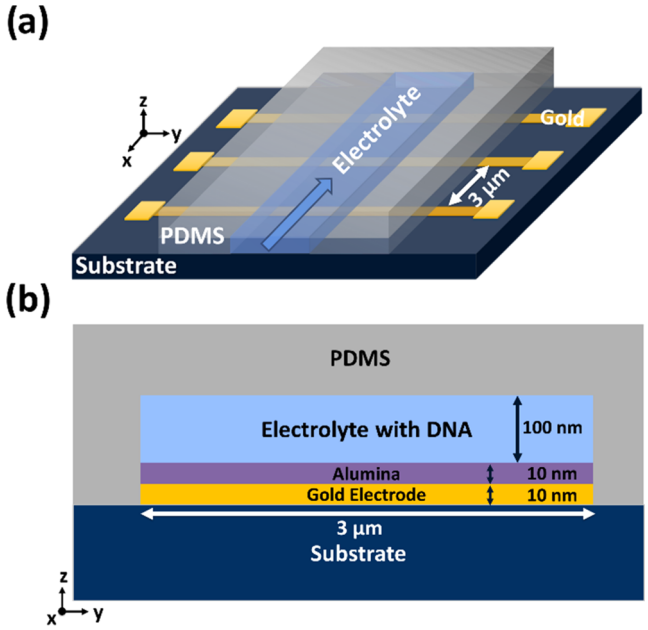

Figure 2. (a) Schematic of the sluice device structure with planar electrodes (in gold) with electrolyte flow along the x-direction. (b) Cross section of the nanotunnel device in the y−z-plane.

configuration, easily integrable with the existing CMOS technology by creating grooves on the substrate *via* the etching process. Apart from the fact that they can be efficiently integrated (align and bond) with nano/microfluidics since they are mechanically robust, they provide higher degrees of freedom and resolution toward manipulating charged macromolecules like DNAs compared to planar structures. Hence, using atomic layer deposition (ALD), conventional lithography, and gas-based etching processes, alumina-based nanotunnels with vertical openings as small as 80−100 nm can be achieved. The strong dependence on the tunnel height to the solution flow resistance may make it challenging to move liquids in channels. Therefore, for the purposes of pumping the solutions containing DNA molecules into the tunnels, it is imperative for the above-mentioned platform to be encapsulated within a micro/nanofluidic circuit.

The integration would require the fabrication of micro/nanofluidic channels on soft polymeric materials like polydimethylsiloxane (PDMS), aligning channels to the on-chip circuit, and bonding the PDMS to the substrate to air seal the channels (preventing leakage). Gold electrodes could also

https://doi.org/10.1021/acsanm.1c02519
ACS Appl. Nano Mater. 2021, 4, 11063−11069

be integrated into these tunnels. Since the height of the tunnel passage needs to be ∼100 nm, the depth of the channel has to be close to 100 nm. To achieve a nanotunnel ∼100 nm in height, a technique such as a vacuum ultraviolet (VUV)-based patterning of PDMS substrate could be implemented to fabricate nanotunnels.

Nanotunnels with Planar Electrodes. To validate the operations of the proposed nanofluidic sluice for DNA data storage, we perform simulation analysis of nanotunnels with planar electrodes, as shown in Figure 2a, to assess the ability of the structure to confine DNA molecules under biased electrodes. In our simulation, the height (z-axis) and width (y-axis) of the tunnels are 100 nm and 3 μm, respectively. We assume that the three 3 μm wide gold electrodes are placed on a substrate, each separated by 3 μm resulting in a tunnel that is 21 μm long. Each of the three gold electrodes is 10 nm in height and is passivated by 10 nm alumina dielectric. The setup could be covered with a soft polymeric material like polydimethylsiloxane (PDMS), for instance, leaving a nanotunnel with a height of 100 nm for the electrolyte with chimeric DNA strands to flow through the channel. One can also assume the presence of electrolyte reservoirs at the beginning and end of the tunnel, as commonly seen with any micro-/nanofluidic devices, but these are not included in the simulation. Figure 2b shows the cross section of the structure in the y−z-plane at an electrode.

Figure 3a shows the two-dimensional (2D) electrostatic potential inside the alumina-passivated nanotunnel for an applied voltage bias of 1 V. The electrolyte concentration inside the tunnels is maintained at 1 mM. As expected, the electric field lines are seen to be directed upward in the tunnel. The electric potential profile along the height of the tunnel (y−z-plane) under the influence ±1 V bias for different electrolyte concentrations are shown in Figure 3b,c. One observes a steep drop in the potential across the dielectric (insulator), whereas the electric potential decreases exponentially from the insulator−electrolyte interface (shown in Figure 3b,c). One estimates that an electrostatic barrier of ∼3−4 K_BT (∼100 mV) is required at the center of the tunnel to effectively control the flow of the DNA. In the case of nanotunnels with planar electrodes, for 1 M concentration solution, one observes that the potential drops down to 0 V within few nanometers from the interface. For lower electrolytic concentrations, such as 10 and 1 mM, the electric potential remains above ∼±100 mV at the center of the tunnel (z = 50 nm). However, the vanishing of the electric potential at the far end (at z = 100 nm) of the tunnel results in a path for the chimeric DNA strands to escape from the tunnel. To overcome these drawbacks, the most promising solution will be to consider an advanced device structure design, where additional electrodes are placed at the top of the tunnels, as described in detail below.

Nanotunnels with Embedded Arch Electrodes. The improved structure design would be similar to the previous nanotunnel structure with planar electrodes but would contain additional arch electrodes at the top of the tunnels, as shown in Figure 4a,b. Here, the covering of the nanotunnels could be made with an alumina coating. A brief schematic illustrating the steps involved in the fabrication of nanotunnels with buried arch electrodes is shown in the Supporting Information Figure S1. Asides from its planar structure, the buried electrode configuration also offers the advantage of stacking the

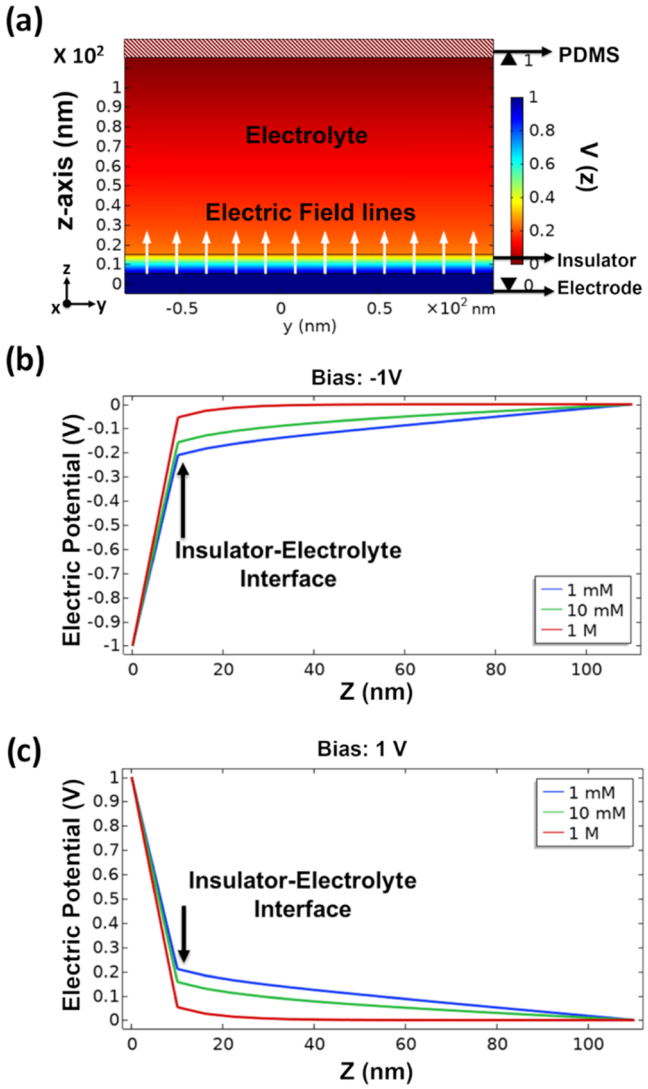

Figure 3. (a) Color plot of the electrostatic potential inside the tunnels in the y−z plane for 1 V applied bias. Electric potential profiles along the height of the tunnel under −1 V (b) and 1 V (c) voltage biases applied at the gold electrodes, respectively.

nanochannels on top of one another for deep integration and its compatibility with CMOS technology.

Figure 4c shows the electrostatic profile inside the tunnel for an applied voltage bias of 1 V with the electrolyte concentration inside the tunnels maintained at 1 mM. One clearly sees that the electric field lines from both electrodes are now directed toward the mid-height of the tunnel. Figure 4d,e displays the electric potential along the height of the tunnel (in the z-direction) for different electrolyte concentrations. Although one observes an exponential decay of the electric potential away from the electrode surface, the electric potential at mid-height of the tunnel remains at approximately ±100 mV for 10 and 1 mM electrolytic solutions because of the voltage applied at the two electrodes positioned at each surface of the tunnel height. This strongly indicates that the DNA motion in these tunnels is effectively influenced by the voltage applied at the electrodes, thereby preventing the leakage of the chimeric DNA strands out of the tunnels, unlike in the previous structure.

https://doi.org/10.1021/acsanm.1c02519
ACS Appl. Nano Mater. 2021, 4, 11063−11069

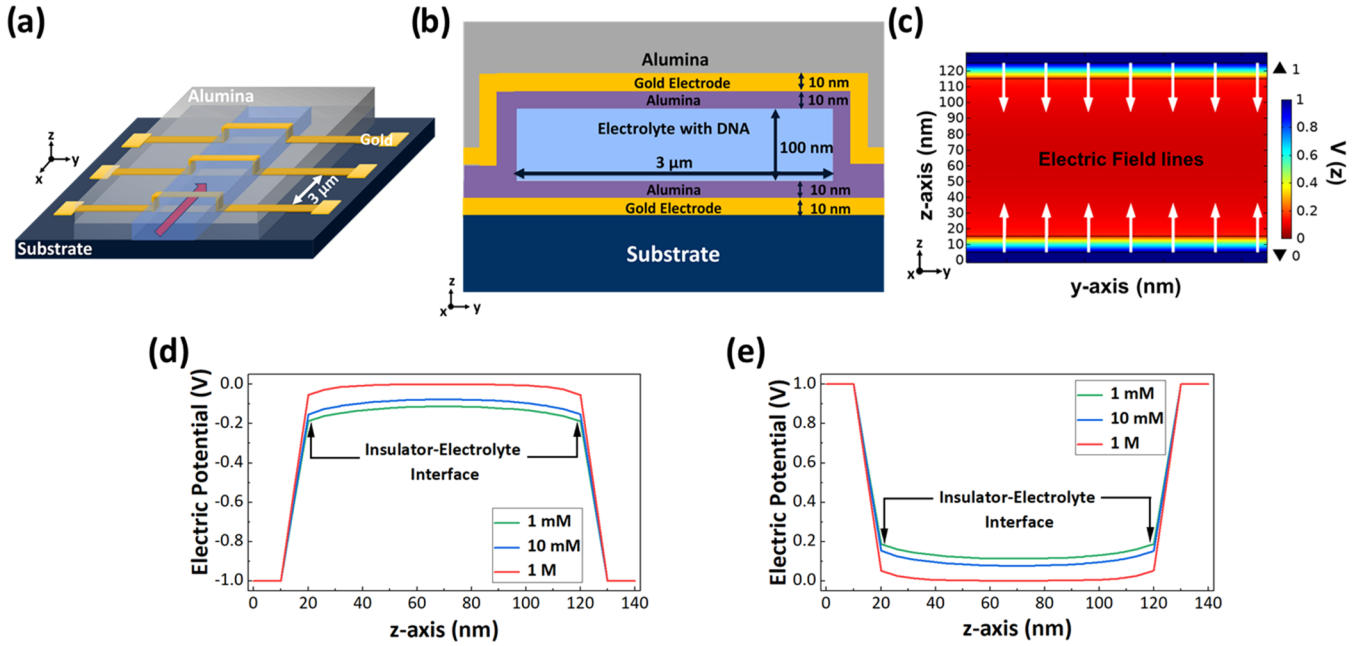

Figure 4. (a) Schematic of the sluice device structure with embedded arch electrodes (in gold) with electrolyte flow along the *x*-direction. (b) Cross section of the nanotunnel device in the *y*−*z*-plane. (c) Color plot of the electrostatic potential inside the tunnels in the *y*−*z*-plane for 1 V applied bias. Electric potential profiles along the height of the tunnel under −1 V (d) and 1 V (e) voltage biases applied at the gold electrodes, respectively.

As shown by Tabatabaei et al., 0.036 bits can be stored in a single DNA base-pair using nicking-based storage (which is similar to what chimeric DNA-based storage can achieve).[18] A single nanofluidic tunnel (5 μm × 5 μm × 100 nm) with a volume of 2.5 μm^3 can store about ∼0.2 GB of data written on 100 bp long DNA strands. This estimated value of 0.2 GB/nanotunnel is calculated considering the sparse distribution of DNA stands inside the tunnels due to electrostatic and van der Waals interactions between the molecules. We can approximately arrange 5500 such tunnels on a 1 cm × 1 cm substrate, giving enough space for the wiring and global contacts. Overall, the proposed CMOS system can store 1.1 TB/cm^2.

Furthermore, the amount of data processed within a second depends on the nanofluidic velocity inside the nanotunnel. The nanofluidic flow velocity has been estimated, both theoretically and experimentally, to be around 10^{-3} m/s.[35−37] Given that the length of a single nanofluidic channel in our proposed device setup is about 21 μm long, one library of chimeric DNA comprising 0.2 GB data can be processed within 21 ms. With a delay of 1 ms between processing each DNA library, ∼10 GB of data can be processed per second. This estimated value is independent of the writing and reading speeds.

Finally, to illustrate the nanofluidic sluice operation of effective capture, hold, and release of chimeric DNA strands through these tunnels, we simulated the sluice operations by applying relevant voltages at each of the three electrodes along the length of the tunnel. Figure 5 shows the plot of electric potential along the entire length of the tunnels (in the *x*-direction) for different concentrations of electrolyte solutions ranging from 1 mM to 1 M. Here, the DNA would flow into the tunnel with the electrolyte under the influence of a pressure gradient created at the two reservoirs at the front and end of the nanotunnel. To capture the chimeric DNA strands into a particular nanotunnel, the first and the middle electrodes of that tunnel are biased with 0.5 and 1 V, respectively, as shown in Figure 5a, so as to attract the inherently negatively charged DNA into the tunnel. A negative bias (−1 V) is applied at the last electrode to repel the DNA strands and force them to stay inside the tunnel during this process. For the hold step, the middle and last electrodes are maintained at 1 and −1 V bias, while the first electrode is biased with −1 V, as shown in Figure 5b. Under a ∼100 mV retaining electrostatic barrier estimate, this ensures that the DNA strands remain in the middle of the tunnels and wait until released for reading. The release process out of the tunnels is then achieved by applying negative voltages at the first and the middle electrodes, as shown in Figure 5c. The last electrode is kept unbiased to maintain a low velocity for the DNA while exiting the tunnels, as higher velocities might cause read errors through a typical solid-state nanopore system.

CONCLUSIONS

In summary, we propose a novel electrically controlled nanofluidic sluice for the effective capture, hold, and release of chimeric DNA strands used in data storage applications. This integrated semiconductor−synthetic biology device offers solutions to many practical challenges such as reduced costs of DNA synthesis and improved component density using chimeric DNA strands, but mainly the nanotunnels' device structures that are compatible with biological entities and easily incorporated with CMOS technology for denser data storage and large-scale integration. Central to our analysis obtained from COMSOL multiphysics simulations is the electrostatic potential distributions inside the nanofluidic channels obtained with planar electrodes versus the use of additional buried arch electrodes that anticipate better DNA retention and release performances than the former structure. There are two possible sources of errors in such a proposed system for DNA data storage: the encoding/decoding errors addressed in detail, including potential solutions by Yazdi et al.[16] and Bornholt et al.,[17] and the errors from the nanofluidic channel itself. The

https://doi.org/10.1021/acsanm.1c02519
ACS Appl. Nano Mater. 2021, 4, 11063−11069

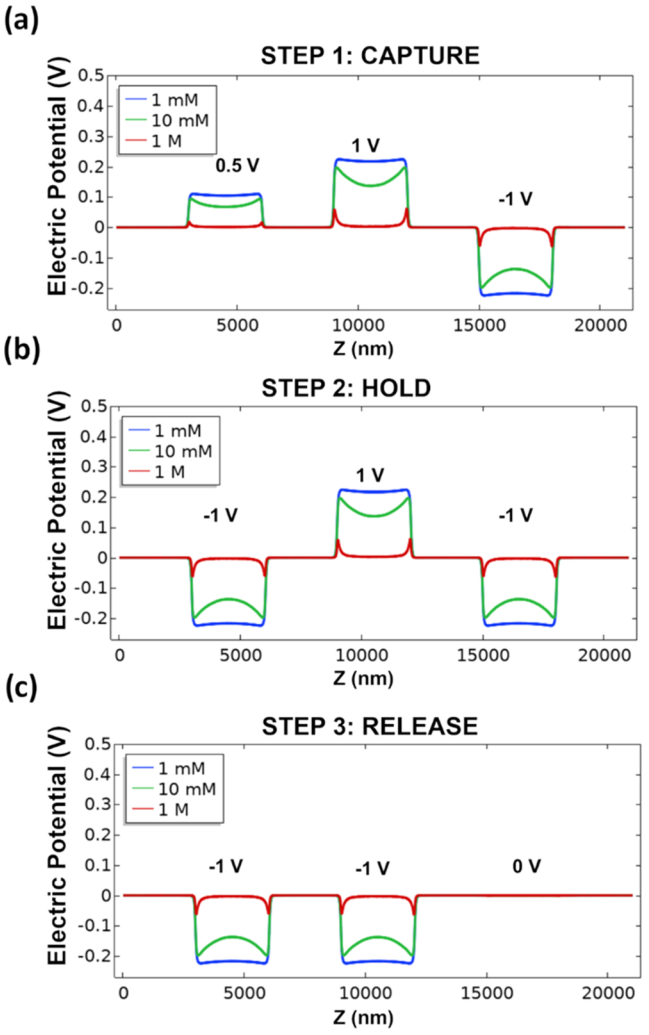

Figure 5. Electric potential profile along the tunnel for various ionic concentration solutions illustrating the three steps of the proposed nanoscale sluice operations: (a) capture, (b) hold, and (c) release of chimeric DNA strands.

errors in the operation of the nanofluidic channel can be easily mitigated by storing multiple copies of the same library in different channels. By doing so, when one channel fails, it can be discarded, which would not affect the operation of the rest of the nanochannel array, while keeping the integrity of the DNA library. Finally, it is expected that the present methodology will be used as a guideline for the design of lab-on-chip devices for DNA-based data storage.

METHODS

We use COMSOL finite element modeling software to simulate the electrically controlled nanofluidic devices with two-dimensional (2D) geometry. The fluxes of electrolytic ions, J_i, in the nanofluidic channel are modeled using the Nernst−Plank equation, described in eq 2

$$J_i = -D_i\nabla c_i - u_{m,i}z_iF_{c_i}\nabla\phi \quad \left[\text{SI unit: } \frac{\text{mol}}{\text{m}^2\cdot\text{s}}\right] \tag{2}$$

where D_i is the diffusion coefficient for ion species i, c_i is the concentration of the polar ions in the electrolyte (i = + or − with z_i = +1 or −1 charge respectively), $u_{m,i}$ is the mobility, F is the Faraday constant, and ϕ is the electric potential obtained from Poisson's equation

$$\nabla\cdot(-\varepsilon\nabla\phi) = \rho \text{ [SI unit: V]} \tag{3}$$

where ε is the relative permittivity and ρ is the charge density, which depends on the ion concentrations as $\rho = F(c_+ - c_-)$.

The outer boundaries of the devices are set to ground condition where ϕ = 0. The ion concentrations are set to their bulk values, which are electroneutral. Additionally, we assume that there are no reactions of the ions in the electrolyte. Hence, the conservation of mass for both ion species requires that $\nabla\cdot J_i = 0$.

To implement Stern theory of double-layer formation,[38] we impose a boundary condition for the electrolyte potential at the electrode interface having a constant Stern layer thickness, λ_S, as

$$\phi + \lambda_S(n\cdot\nabla\phi) = \phi_M \tag{4}$$

where n is the unit vector normal to the electrode surface and ϕ_M is the potential applied at the electrode.

ASSOCIATED CONTENT

Supporting Information

The Supporting Information is available free of charge at https://pubs.acs.org/doi/10.1021/acsanm.1c02519.

Fabrication steps of a nanotunnel device with buried arch electrodes (PDF)

AUTHOR INFORMATION

Corresponding Author

Jean-Pierre Leburton − *Department of Electrical and Computer Engineering, Holonyak Micro and Nanotechnology Laboratory, and Department of Physics, University of Illinois at Urbana-Champaign, Urbana, Illinois 61801, United States;* orcid.org/0000-0002-8183-5581; Phone: (217) 333-6813; Email: jleburto@illinois.edu

Authors

Nagendra Athreya − *Department of Electrical and Computer Engineering and Holonyak Micro and Nanotechnology Laboratory, University of Illinois at Urbana-Champaign, Urbana, Illinois 61801, United States*

Apratim Khandelwal − *Department of Electrical and Computer Engineering and Holonyak Micro and Nanotechnology Laboratory, University of Illinois at Urbana-Champaign, Urbana, Illinois 61801, United States*

Xiuling Li − *Department of Electrical and Computer Engineering and Holonyak Micro and Nanotechnology Laboratory, University of Illinois at Urbana-Champaign, Urbana, Illinois 61801, United States;* orcid.org/0000-0003-3698-5182

Complete contact information is available at: https://pubs.acs.org/10.1021/acsanm.1c02519

Author Contributions

N.A. and J.-P.L. conceived the presented idea. N.A. designed and performed the computations and analyses with J.-P.L.'s contribution upon A.K.'s and X.L.'s technical suggestions. The manuscript was written through contributions of all authors. All authors have given approval to the final version of the manuscript.

Funding

This work is supported by grants from National Science Foundation (NSF CCF 18-07526) and Semiconductor Research Corporation (SRC 2018-SB-2839).

Notes

The authors declare no competing financial interest.

■ ACKNOWLEDGMENTS

The authors are indebted to Prof. Olgica Milenkovic and Prof. Charles Schroeder for their helpful discussions and the computing resources offered by The Visualization Laboratory at Beckman Institute for Advanced Science and Technology.

■ REFERENCES

(1) Feynman, R. P. *There's Plenty of Room at the Bottom*; Engineering and Science; CRC Press, 1960; Vol. *23*, pp 22−36.
(2) Church, G. M.; Gao, Y.; Kosuri, S. Next-Generation Digital Information Storage in DNA. *Science* **2012**, *337*, No. 1628.
(3) Goldman, N.; Bertone, P.; Chen, S.; Dessimoz, C.; LeProust, E. M.; Sipos, B.; Birney, E. Towards Practical, High-Capacity, Low-Maintenance Information Storage in Synthesized DNA. *Nature* **2013**, *494*, 77−80.
(4) Yong, E. Synthetic Double-Helix Faithfully Stores Shakespeare's Sonnets. *Nature* **2013**, No. 12279.
(5) Grass, R. N.; Heckel, R.; Puddu, M.; Paunescu, D.; Stark, W. J. Robust Chemical Preservation of Digital Information on DNA in Silica with Error-Correcting Codes. *Angew. Chem., Int. Ed.* **2015**, *54*, 2552−2555.
(6) Choi, H.; Choi, Y.; Choi, J.; Lee, A. C.; Yeom, H.; Hyun, J.; Ryu, T.; Kwon, S. Purification of Multiplex Oligonucleotide Libraries by Synthesis and Selection. *Nat. Biotechnol.* **2021**, *432*, No. 1050.
(7) Pinto, A.; Chen, S. X.; Zhang, D. Y. Simultaneous and Stoichiometric Purification of Hundreds of Oligonucleotides. *Nat. Commun.* **2018**, *9*, No. 2467.
(8) Deamer, D.; Akeson, M.; Branton, D. Three Decades of Nanopore Sequencing. *Nat. Biotechnol.* **2016**, *34*, 518−524.
(9) Dekker, C. Solid-State Nanopores. *Nat. Nanotechnol.* **2007**, *2*, 209−215.
(10) Gracheva, M. E.; Xiong, A.; Aksimentiev, A.; Schulten, K.; Timp, G.; Leburton, J.-P. Simulation of the Electric Response of DNA Translocation through a Semiconductor Nanopore−Capacitor. *Nanotechnology* **2006**, *17*, 622−633.
(11) Athreya, N. B. M.; Sarathy, A.; Leburton, J. P. Large Scale Parallel DNA Detection by Two-Dimensional Solid-State Multipore Systems. *ACS Sens.* **2018**, *3*, 1032−1039.
(12) Choi, Y.; Bae, H. J.; Lee, A. C.; Choi, H.; Lee, D.; Ryu, T.; Hyun, J.; Kim, S.; Kim, H.; Song, S.-H.; Kim, K.; Park, W.; Kwon, S. DNA Micro-Disks for the Management of DNA-Based Data Storage with Index and Write-Once−Read-Many (WORM) Memory Features. *Adv. Mater.* **2020**, *32*, No. 2001249.
(13) Banal, J. L.; Shepherd, T. R.; Berleant, J.; Huang, H.; Reyes, M.; Ackerman, C. M.; Blainey, P. C.; Bathe, M. Random Access DNA Memory Using Boolean Search in an Archival File Storage System. *Nat. Mater.* **2021**, *20*, 1272−1280.
(14) Yazdi, S. M. H. T.; Yuan, Y.; Ma, J.; Zhao, H.; Milenkovic, O. A Rewritable, Random-Access DNA-Based Storage System. *Sci. Rep.* **2015**, *5*, No. 14138.
(15) Organick, L.; Ang, S. D.; Chen, Y.-J.; Lopez, R.; Yekhanin, S.; Makarychev, K.; Racz, M. Z.; Kamath, G.; Gopalan, P.; Nguyen, B.; Takahashi, C. N.; Newman, S.; Parker, H.-Y.; Rashtchian, C.; Stewart, K.; Gupta, G.; Carlson, R.; Mulligan, J.; Carmean, D.; Seelig, G.; Ceze, L.; Strauss, K. Random Access in Large-Scale DNA Data Storage. *Nat. Biotechnol.* **2018**, *36*, 242−248.
(16) Yazdi, S. M. H. T.; Gabrys, R.; Milenkovic, O. Portable and Error-Free DNA-Based Data Storage. *Sci. Rep.* **2017**, *7*, No. 5011.
(17) Bornholt, J.; Lopez, R.; Carmean, D.; Ceze, L.; Seelig, G.; Strauss, K. In *A DNA-Based Archival Storage System*, ASPLOS 2016 (International Conference on Architectural Support for Programming Languages and Operating Systems); Association for Computing Machinery, 2016.
(18) Tabatabaei, S. K.; Wang, B.; Athreya, N. B. M.; Enghiad, B.; Hernandez, A. G.; Fields, C. J.; Leburton, J.-P.; Soloveichik, D.; Zhao, H.; Milenkovic, O. DNA Punch Cards for Storing Data on Native DNA Sequences via Enzymatic Nicking. *Nat. Commun.* **2020**, *11*, No. 1742.
(19) Erlich, Y.; Zielinski, D. DNA Fountain Enables a Robust and Efficient Storage Architecture. *Science* **2017**, *355*, 950−954.
(20) Heckel, R.; Shomorony, I.; Ramchandran, K.; David, N. In *Fundamental Limits of DNA Storage Systems*, 2017 IEEE International Symposium on Information Theory (ISIT); IEEE, 2017; pp 3130−3134.
(21) Jang, J.; Kim, H.-S.; Cho, W.; Cho, H.; Kim, J.; Shim, S. I.; Younggoan; Jeong, J.-H.; Son, B.-K.; Kim, D. W.; Kihyun; Shim, J.-J.; Lim, J. S.; Kim, K.-H.; Yi, S. Y.; Lim, J.-Y.; Chung, D.; Moon, H.-C.; Hwang, S.; Lee, J.-W.; Son, Y.-H.; Chung, U.-I.; Lee, W.-S. In *Vertical Cell Array Using TCAT(Terabit Cell Array Transistor) Technology for Ultra High Density NAND Flash Memory*, 2009 Symposium on VLSI Technology; IEEE, 2009; pp 192−193.
(22) Laure, C.; Karamessini, D.; Milenkovic, O.; Charles, L.; Lutz, J.-F. Coding in 2D: Using Intentional Dispersity to Enhance the Information Capacity of Sequence-Coded Polymer Barcodes. *Angew. Chem., Int. Ed.* **2016**, *55*, 10722−10725.
(23) Lutz, J.-F.; Ouchi, M.; Liu, D. R.; Sawamoto, M. Sequence-Controlled Polymers. *Science* **2013**, *341*, No. 1238149.
(24) Roy, R. K.; Meszynska, A.; Laure, C.; Charles, L.; Verchin, C.; Lutz, J.-F. Design and Synthesis of Digitally Encoded Polymers That Can Be Decoded and Erased. *Nat. Commun.* **2015**, *6*, No. 7237.
(25) Athreya, N.; Milenkovic, O.; Leburton, J.-P. Interaction Dynamics and Site-Specific Electronic Recognition of DNA-Nicks with 2D Solid-State Nanopores. *npj 2D Mater. Appl.* **2020**, *4*, No. 32.
(26) Sarathy, A.; Qiu, H.; Leburton, J. P. Graphene Nanopores for Electronic Recognition of DNA Methylation. *J. Phys. Chem. B* **2017**, *121*, 3757−3763.
(27) Sarathy, A.; Athreya, N. B.; Varshney, L. R.; Leburton, J.-P. Classification of Epigenetic Biomarkers with Atomically Thin Nanopores. *J. Phys. Chem. Lett.* **2018**, *9*, 5718−5725.
(28) Li, X. Self-Rolled-up Microtube Ring Resonators: A Review of Geometrical and Resonant Properties. *Adv. Opt. Photonics* **2011**, *3*, 366−387.
(29) Prinz, V. Y.; Seleznev, V. A.; Gutakovsky, A. K.; Chehovskiy, A. V.; Preobrazhenskii, V. V.; Putyato, M. A.; Gavrilova, T. A. Free-Standing and Overgrown InGaAs/GaAs Nanotubes, Nanohelices and Their Arrays. *Phys. E* **2000**, *6*, 828−831.
(30) Li, C.; Li, L.; Petukh, M.; Alexov, E. Progress in Developing Poisson-Boltzmann Equation Solvers. *Comput. Math. Biophys.* **2013**, *1*, 42−62.
(31) Matange, K.; Tuck, J. M.; Keung, A. J. DNA Stability: A Central Design Consideration for DNA Data Storage Systems. *Nat. Commun.* **2021**, *12*, No. 1358.
(32) Anchordoquy, T. J.; Molina, M. C. Preservation of DNA. *Cell Preserv. Technol.* **2007**, *5*, 180−188.
(33) AlRokayan, S. A. Effect of Storage Temperature on the Quality and Quantity of DNA Extracted from Blood. *Pak. J. Biol. Sci.* **2000**, *3*, 392−394.
(34) Baoutina, A.; Bhat, S.; Partis, L.; Emslie, K. R. Storage Stability of Solutions of DNA Standards. *Anal. Chem.* **2019**, *91*, 12268−12274.
(35) Brites, C. D. S.; Xie, X.; Debasu, M. L.; Qin, X.; Chen, R.; Huang, W.; Rocha, J.; Liu, X.; Carlos, L. D. Instantaneous Ballistic Velocity of Suspended Brownian Nanocrystals Measured by Upconversion Nanothermometry. *Nat. Nanotechnol.* **2016**, *11*, 851−856.
(36) Kanjirakat, A.; Sadr, R. Near-Wall Velocity Profile Measurement for Nanofluids. *AIP Adv.* **2016**, *6*, No. 015308.
(37) Gupta, C.; Liao, W.-C.; Gallego-Perez, D.; Castro, C. E.; Lee, L. J. DNA Translocation through Short Nanofluidic Channels under Asymmetric Pulsed Electric Field. *Biomicrofluidics* **2014**, *8*, No. 024114.
(38) Stern, O. Zur Theorie Der Elektrolytischen Doppelschicht. *Z. Elektrochem. Angew. Phys. Chem.* **1924**, *30*, 508−516.

https://doi.org/10.1021/acsanm.1c02519
ACS Appl. Nano Mater. 2021, 4, 11063−11069